Materials Today Communications 33 (2022) 104914

Contents lists available at ScienceDirect

Materials Today Communications

journal homepage: www.elsevier.com/locate/mtcomm

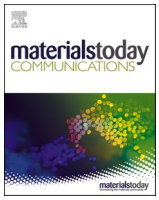

Texture and microstructural changes after thermal cycling of 6061Al-20vol %SiC_w metal matrix composite: The role of microscopic internal stresses

M. Eddahbi [a], R. Fernández [b], I. Llorente [b], G. González-Doncel [b,*]

[a] Department of Physics, Universidad Carlos III, Leganes 28911, Madrid, Spain
[b] Department of Physical Metallurgy, Centro Nacional de Investigaciones Metalúrgicas (CENIM), C.S.I.C., Av. de Gregorio del Amo 8, 28040 Madrid, Spain

ARTICLE INFO

Keywords:
Metal matrix composites
Thermal cycling
Texture
Microstructure
Microscopic internal stresses

ABSTRACT

The dramatic texture and microstructural changes observed in 6061Al-20vol%SiC_w metal matrix composite undergoing severe thermal cycles, under the absence and the simultaneous action of an external tensile stress, are studied. Under only thermal cycles (100–450 °C) homogenization and disorientation of the SiC whisker reinforcement and crystallographic texture randomization occurs. However, when a simultaneous tensile stress is applied, the whiskers rotate so that their long direction aligns with the tensile axes. Furthermore, a strong texture and large deformations (superplasticity), higher than 1000%, are achieved. These results are explained on the basis of the microscopic stress fields generated at the different microstructural scales (stresses of type II and type III) and well-known observation of dislocation generation at the SiC-metal interface during the cooling period of the cycles. We propose that moving dislocations (responsible of type III stresses) operate differently under the absence or the presence of the external stress. Under no stress, dislocation motion (occurring mainly during the heating period) is driven only by the type II internal stress. However, dislocation motion is improved when an external stress is applied, leading to texture changes and large elongations. Despite that a low external stress is applied, it overcomes the effect of the internal stresses for dislocation motion.

1. Introduction

Nowadays, it can be said that metal matrix composites, MMCs, which emerged in the 1970 s and 1980 s of the past century creating great expectations, have reached maturity. These materials have outstanding mechanical properties compared to their corresponding metallic matrices; They have improved mechanical properties at both room [1] and elevated [2,3] temperatures, better wear resistance [4,5], and thermal stability [6]. Possibly, the only barrier to their everyday use, *e.g.*, in the transport and energy industrial sectors, is their still limited competitive manufacturing costs [7].

The potential use of MMCs includes not only applications at high and steady temperatures (isothermal conditions) but also uses in which changing temperature (thermal cycling) conditions, such as in some engine parts, can be relevant [8]. Although their good isothermal creep behavior has been demonstrated [2,3], it is important to note that when the experimental conditions involve severe temperature changes, the tensile behavior of MMCs undergoes dramatic changes, as it has been shown in several investigations [8–13]. In summary, these materials deform under very low applied stresses, but at relatively high strain rates, in comparison to deformation behavior under isothermal creep conditions. A transient creep (primary creep region) is not manifested and, rather, the strain rate is found to be constant with increasing strain.

In addition, they may also experience very large deformations, exceeding 1000% tensile elongation: *i.e.*, superplasticity is achieved [14–16]. This kind of superplasticity is usually referred to as internal stress superplasticity [15–17], ISS. It differs from the as known "structural superplasticity" (which occurs under isothermal conditions), where grain boundary sliding, GBS, is well accepted to be the dominant deformation mechanism [17–19]. On the contrary, the deformation mechanisms responsible of ISS in MMCs have not yet been fully investigated, though the internal stresses may play a crucial role. One must consider that different types of internal stresses (at different scales) can be developed in MMCs [20]. However, the way these stresses evolve during the thermal cycles is described in a rather general and ambiguous manner [12].

The dominance of the GBS mechanism in structural superplasticity is supported, for example, by crystallographic texture randomization induced by grain rotation during deformation. Grain rotation implies that grains, initially possessing a common crystallographic orientation

* Corresponding author.
E-mail address: ggd@cenim.csic.es (G. González-Doncel).

https://doi.org/10.1016/j.mtcomm.2022.104914
Received 9 February 2022; Received in revised form 30 October 2022; Accepted 9 November 2022
Available online 11 November 2022

with the tensile axis, tend to reorient differently from each other with increasing strain, a phenomenon which leads to texture intensity decrease [18,19]. In contrast, and despite the above studies on the thermal cycling creep behavior of MMCs, it is surprising that analyses from the point of view of the crystallographic texture changes are still scarce and incomplete [21,22]. Texture evolution has shown itself to be a powerful tool for investigating not only microstructural changes of materials undergoing different thermomechanical treatments, but also the underlying mechanisms responsible for them [23–25]. The texture/microstructure changes observed in the present work will be explained within the framework of the microscopic internal stress fields generated as a consequence of the large difference in the coefficient of the thermal expansion (CTE) between the matrix and the reinforcement (of about 6:1 in this composite). Conventionally, these stresses, developed at different microstructural scales, are referred to as microscopic residual stresses, m-RS, as long as they remain in the material after a thermomechanical treatment [20]. In the present case, however, they will be called internal (non-residual) stresses due to the drastic changes that they are proposed to undergo during thermal cycling.

In summary, the purpose of the present study is to explain the microstructural and crystallographic texture changes observed in powder metallurgical, PM, 6061Al-20vol%SiC_w composite when it undergoes repeated and severe thermal cycles and also when a tensile load is applied during the thermal cycles. It must be kept in mind that despite their outstanding properties, the dramatic different mechanical behavior of MMCs between isothermal *vs.* thermal cycling conditions can be a serious drawback in the design of structural components operating in situations where temperature variations may occur. In particular, when an external load is applied during the thermal cycles [9]. For this reason, their behavior under these conditions needs further attention.

2. Material and experimental details

The material investigated is 6061Al-20vol%SiC_w MMC. It was manufactured in the form of a back-extruded tube by a PM route. The manufacture procedure is sketched in Fig. 1. Briefly, the procedure consists of first mixing the commercial aluminum alloy powder with the SiC_w of 1 μm in diameter and 10 in aspect ratio. The powder mixture is then hot compacted using the appropriate tools, Fig. 1A). Finally, the powder compact, Fig. 1B), is progressively back-extruded, as shown in Fig. 1C) and D). Dimensions of the final tube, Fig. 1E), were 152.5 mm in diameter with 12.7 mm wall thickness. Details of the tensile sample dimensions and the thermal cycling tests are described in [15]. Tests were conducted on samples machined with the tensile axis direction parallel to the extrusion, E, and transverse, T, directions, consistently with the reference system sketched in Fig. 1E). Thermal cycling tests were carried out under controlled constant stress conditions, while the temperature oscillated in the interval of 100–450 °C in a period time of 200 s [15]. For the present study, a longitudinal sample tested at 10 MPa and a transverse one tested at 7 MPa were selected for microstructural characterization. The strain rates achieved were, approximately, of 5×10^{-6} s^{-1} and 3×10^{-6} s^{-1}, respectively.

Metallographical analysis was conducted using TENEO-FEI scanning electron microscopy, SEM, and optical microscopy, OM, after appropriate sample surface preparation, using conventional metallographical procedures. These samples were taken from sections of the original tube and the thermally cycled samples. The observations correspond, therefore, to the bulk microstructure of the composite after the different conditions.

Finally, texture measurements were performed using a Bruker AXS D8 diffractometer equipped with a Co-Kα X-ray tube with Goebel mirror optics and a LynxEye linear position-sensitive detector in 0D/high resolution mode. These measurements were completed on, both, the Al alloy and the SiC_w reinforcing phases. Pole figures {111}, {200}, {220}, and {311} for the Al alloy phase and {111}, {220}, and {311} and for the SiC_w reinforcing phase were obtained over azimuthal angles χ ranging from 0° to 75° in step mode. For both polar coordinates, χ and φ, measurements at increments of Δ(χ, φ)= 5° were taken to cover all possible spatial sample orientations. A texture-less standard sample of pure Al was used for defocusing correction. Quantitative three-dimensional orientation distribution functions, ODF (or $f(g)$ where g is the orientation in the Euler's space given by Euler angles φ_1, Φ, and φ_2), were obtained using the series expansion method (l_{max}=22). The ODFs were represented with iso-intensity lines in equidistant sections, $\Delta\varphi_2 = 5°$, in the Euler's space. The quantitative texture analysis and the representation of pole figures and ODF- $f(g)$ were carried out using the MATLAB toolbox MTEX software [26]. Since the short SiC_w whiskers are single crystals (FCC structure) with the ⟨111⟩ crystallographic direction parallel to the long whisker direction, macro-texture analysis of this phase provides direct quantitative information (completer and more reliable than SEM or OM) of the overall 3D whisker alignment in the aluminum matrix, similarly as in [27].

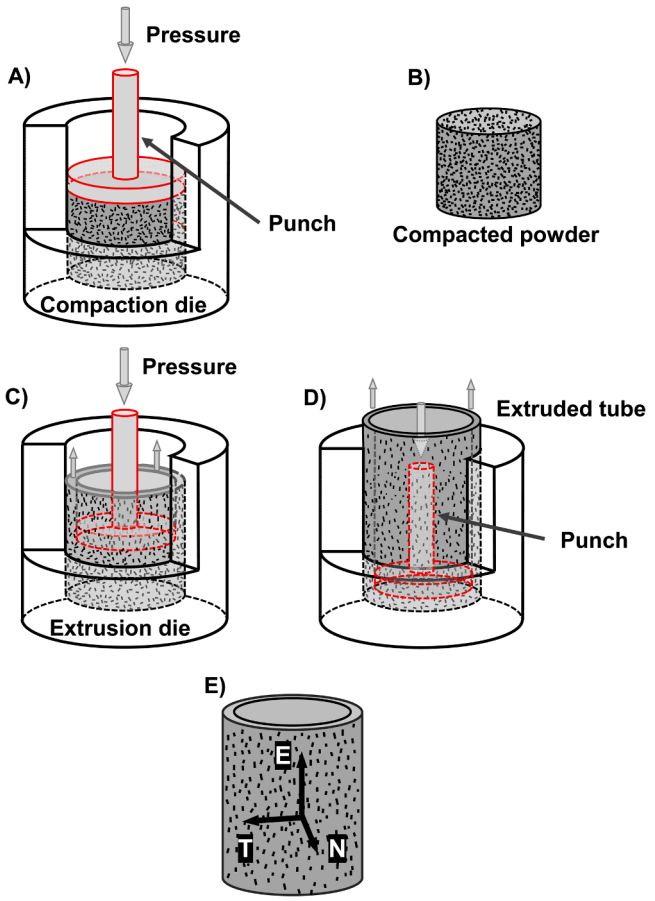

Fig. 1. Scheme of the PM manufacturing process of the extruded MMC tube. A) Compaction of the Al alloy and SiC powder blend. B) Resulting green compacted powder. C) and D) Back-extrusion process of the compacted blend. E) Final consolidated MMC tube showing the cylindrical coordinate system.

3. Results

The microstructure of the composite has been briefly outlined previously [15]. In the present study, both the microstructure and texture are described in detail (see Figs. 2 and 3). In Fig. 2, a reasonable homogeneous distribution of the SiC_w in the metallic matrix, similar to that observed in other investigations [28], is revealed. Some whisker-free regions, however, can also be observed. These regions, indicated by arrows in Fig. 2A) and B) and also observed in the high magnification micrographs of Fig. 2C) and D), are characterized by being elongated

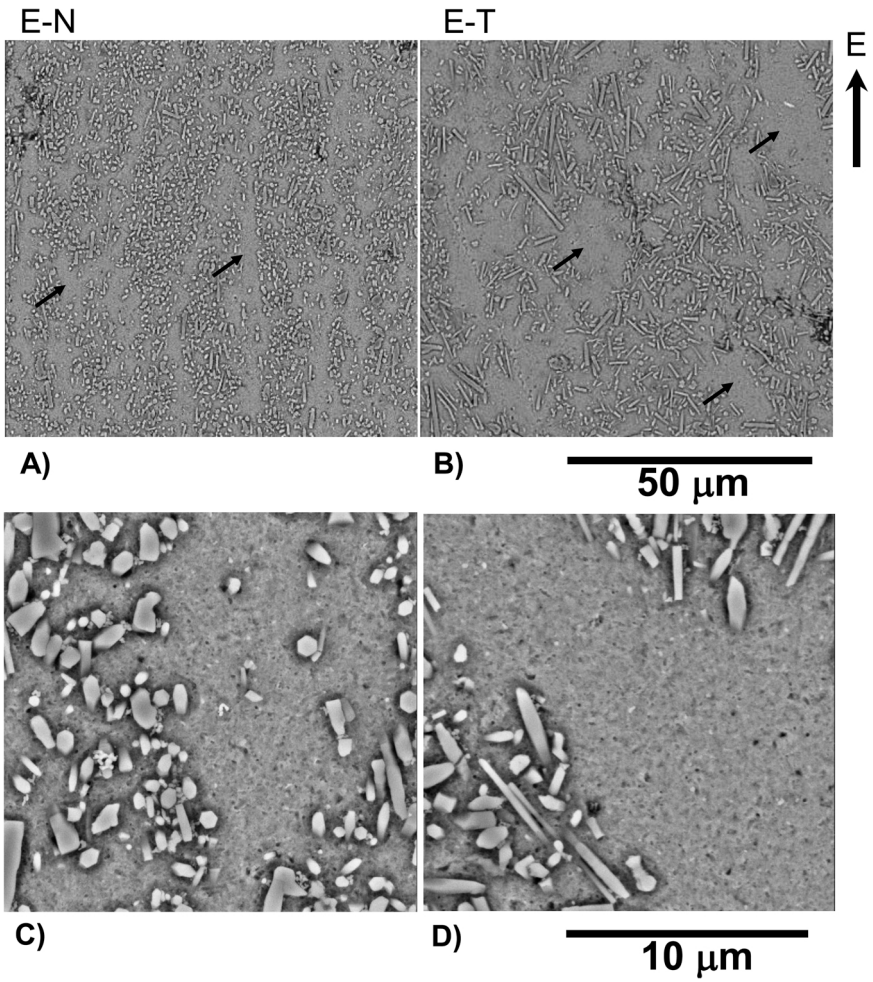

Fig. 2. Metallographical sections showing the distribution of the SiC_w reinforcement in the interior of the as-extruded tube. A) E-N section showing elongated whisker-free regions (see arrows) parallel to E direction. B) E-T section showing wider whisker-free regions (arrows), also parallel to E direction. C) and D) High magnification micrographs of both sections with a detail of whisker-free regions.

when viewed from E-N cuts, Fig. 2A), but more rounded from an E-T section, Fig. 2B). From these views, it is inferred that they are elongated wafer shaped regions, in which the long direction is parallel to E while the short one is parallel to N. The presence of free-whisker regions in MMCs is normal, and is a consequence of the difficulty in achieving a complete uniformity of the reinforcing phase during composite manufacturing [28,29]. On the other hand, the plastic flow triggered by the extrusion process causes the tendency to the short whiskers to be slightly aligned with E direction and placed preferably on the E-T plane.

The crystallographic texture of the Al alloy and SiC_w phases is not too strong. It is summarized in the $f(g)$ *vs.* φ_2 plot of Fig. 3A). For the Al alloy phase it can be described by a combination of the Goss orientation (G) $\{110\}\langle 001\rangle$, which lays in the α − fiber, and the $\{113\}\langle 332\rangle + \{531\}\langle 112\rangle$ orientations, which lay in the β-fiber, close to Copper (Cu), $\{112\}\langle 111\rangle$, and S, $\{123\}\langle 346\rangle$ or $\{124\}\langle 112\rangle$, orientations. Except for the absence of the Brass (Bs) orientation, $\{110\}< 112 >$, these fibers are typical of aluminum alloys processed by rolling [30–33]. The above one is a significant finding which reveals that the constraint imposed by the back-extrusion process to obtain the tube is similar to that of a rolling one. In this framework, the extrusion direction, E in Fig. 1, would be equivalent to the rolling one and, similarly, N and T to the normal and transverse directions, respectively. This is consistent with the idea that a plain strain condition (with E-N in Fig. 1 the deformation plane) is imposed to the back extruded tube. Fig. 3B) reveals the rolled-like texture in the form of a 111-pole figure of the metallic matrix. The weak texture is most likely due to the presence of the reinforcing phase, which prevents the development of a strong deformation texture. In other words, the un-deformable SiC_w facilitate the formation of new recrystallized grains (randomly oriented) by a particle-stimulated-nucleation, PSN, mechanism [27,34].

On the other hand, the texture of the SiC_w phase is consistent with the microstructural observations, Fig. 2. As shown by the 111-pole figure, Fig. 3C), the maximum intensity (1.7 times the random one) is obtained along E direction. Similar to the Al alloy phase, the texture intensity of the SiC_w is quite low. The tendency of the SiC_w to be aligned with E is consistent with the deformation suffered by the material (similar to a rolling process). These results show that the short SiC_w, initially randomly oriented in the green powder compact, tend to realign with E during the back-extrusion process [15].

Two important findings are seen when the composite material undergoes repeated cycles (about 2000). The results are visible from Figs. 4 and 5, where the microstructure and the texture, respectively, are shown. Firstly, it can be seen from Fig. 4 that the original whisker-free regions, as viewed from section E-T, vanish, revealing that the SiC_w have, literally, moved in the Al alloy matrix, filling in these regions. Secondly, the initial low texture intensity of, both, the Al alloy and SiC_w phases diminishes becoming nearly random. As it will be discussed, these results can be interpreted from the evolution and interaction between the microscopic internal stress fields developed in the composite.

When, additionally, an external stress is applied (and superplasticity is achieved), the changes are even more accentuated. This can be seen in Figs. 6 and 7, where the microstructure and the texture, respectively, of

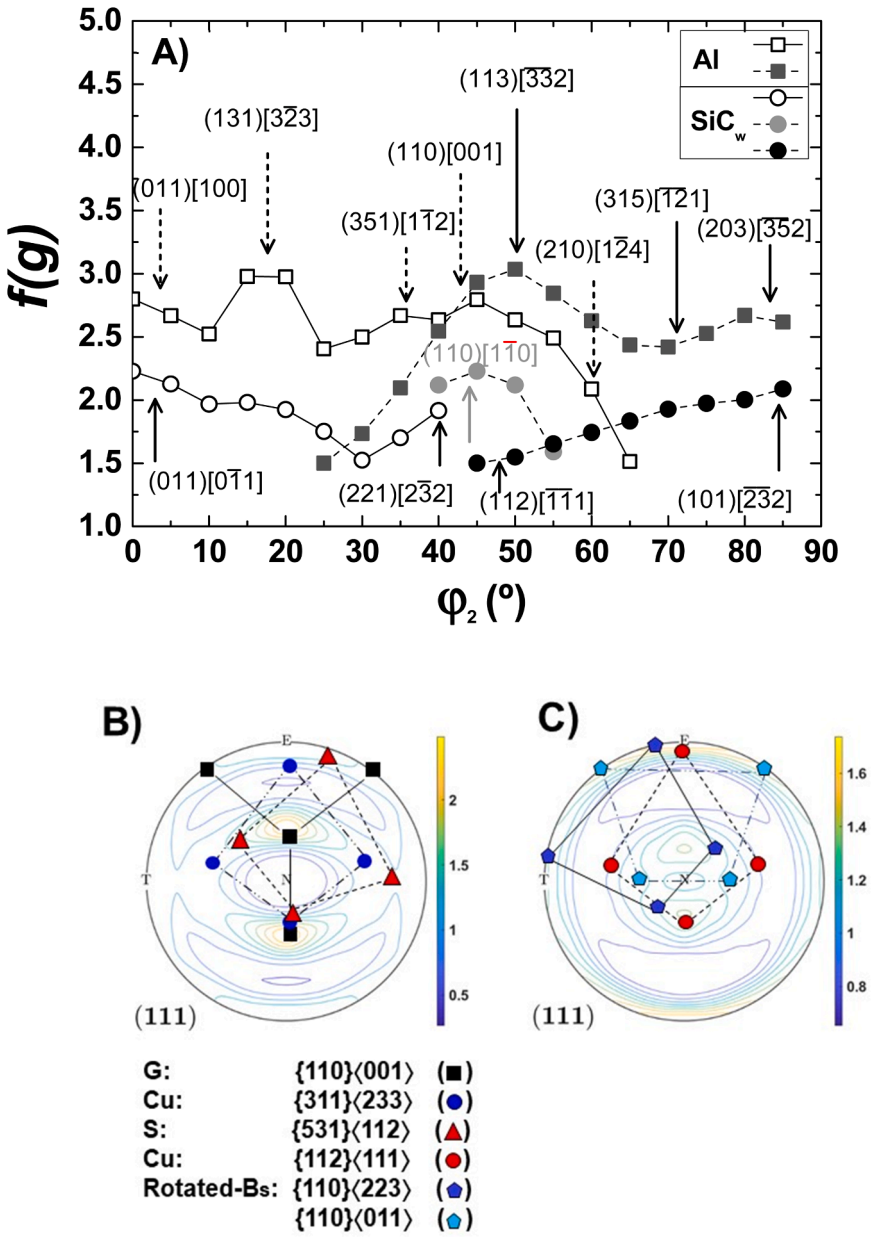

Fig. 3. Texture of the as received composite material. A) Variation of the ODF intensity, *f(g)*, with Euler angle φ_2 showing the β fiber of the Al alloy phase and the orientations of the ceramic reinforcement. B) 111 pole figure revealing the slight trend of the crystallographic ⟨111⟩ matrix grains to be oriented parallel to E direction. C) 111 pole figure revealing the slight alignment of the SiC_w with E direction.

samples which have been pulled along directions E and T, are shown. Fig. 6A) and B) show the alignment of the SiC_w in samples pulled along E and T, respectively (the tensile axis in each case is indicated by arrows). In both cases, a rotation of the SiC_w long direction towards the external applied stress axes is produced. This result is the opposite to what it is obtained with only thermal cycles, Figs. 4 and 5. The SiC_w realignment with the tensile axes and the homogenization process take place simultaneously. Fig. 6C) is an example of the extremely high tensile elongations (> 1000%) achieved under these thermal cycling conditions. Large tensile elongations and whisker alignment with the tensile axis direction have been reported in previous studies on MMCs pulled under thermal cycling conditions [22].

Fig. 7 summarizes the texture, in the form of 111 pole figures for the metallic and ceramic phases of the thermally cycled composite samples stretched along E, Fig. 7A) and B), and T axis, Fig. 7C) and D). Now, a clear increase of texture intensity occurs. Texture of the matrix phase, Fig. 7A) and C), reveals that a significant amount of grains rotated to accommodate the crystallographic ⟨111⟩ with the tensile axis direction. On the other hand, pole figures of Fig. 7B) and D) (corresponding to the reinforcement), also accentuate the intensity in the tensile axis direction, consistent with the whisker reorientation, Fig. 6. The texture increase revealed by Fig. 7A and C) accounts for a strong dislocation motion activity in the absence of strain hardening. Dislocation motion on FCC slip systems provokes lattice grain rotation such that the crystallographic ⟨111⟩ aligns with the tensile axes.

In summary, the most relevant result derived from the texture measurements is that the crystallographic ⟨111⟩ of the Al grains rotates towards the tensile axis direction, regardless its orientation with the sample reference system. This is opposite to the observed texture decay after conventional superplastic deformation where GBS dominates the large elongations achieved. The texture intensity increase can be correlated with the microscopic internal stresses developed and the

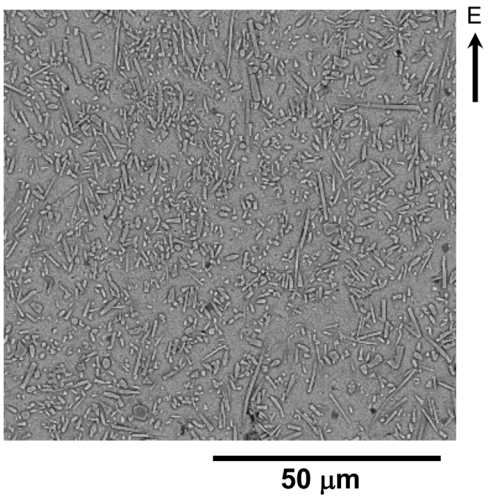

Fig. 4. Microstructure of the 6061Al-20vol%SiC_w composite material (section E-T) showing the reinforcement distribution in the metallic matrix after thermal cycling. The initial whisker-free regions visible in the original microstructure (Fig. 2) have virtually disappeared.

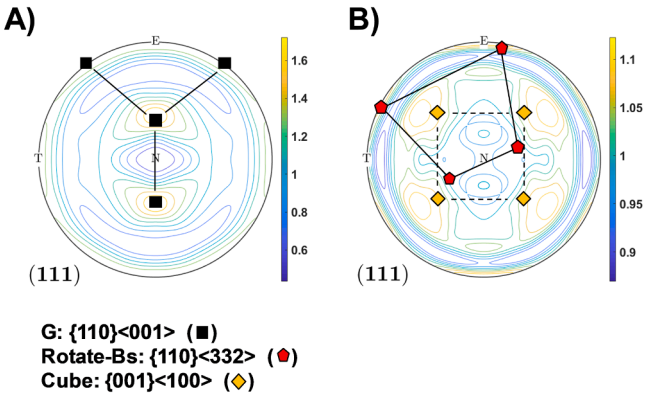

Fig. 5. Texture of the thermally-cycled 6061Al-20vol%SiC_w composite material. A) 111 pole figure of the Al alloy matrix showing orientation spread around N direction and emergence of G orientation. B) 111 pole figure of the SiC_w reinforcement revealing their tendency to reduce texture intensity and whisker alignment.

motion of a high amount of dislocations, as it will be discussed in the next section.

Understanding in depth the specific changes of the texture components observed between the initial state, Fig. 3, and those resulting from repeated thermal cycles, in the absence, Fig. 5, and under the simultaneous action of the external load, Fig. 7, is complex and is beyond the scope of this study. This work, which is based on the analysis of the ODFs obtained in each case, is under progress and will be the subject of future publication.

Finally, it is worth mentioning that the dramatic microstructural changes observed in this composite after thermal cycling conditions is contrary to the general high microstructural stability of MMCs after isothermal treatments [35,36]. This is associated with a dislocation generation process at the metal-ceramic interface, to the interaction between microscopic stresses, and also to the inhibition of a dislocation pinning effect. All this will be treated in the next section.

4. Discussion

The observed texture changes will allow explaining the thermal cycling behavior of MMCs on the basis of the evolution of the microscopic internal stress fields and their interaction with the dislocations. As mentioned, the importance of dislocation motion and the internal stresses has been suggested to account for this behavior. However, a complete and thorough description of the thermal cycling behavior of MMCs is, surprisingly, still absent [12,13].

As known, m-RS in MMCs are developed not only between matrix and reinforcing phases (within a scale ranging in the order of some few μm) [20]. Microscopic stresses are also generated at a much lower scale, that of the distance between lattice defects; *i.e.*, in the order of nanometers (*e.g.*, the distance between dislocations) [37]. The first one, which originates as a consequence of the different CTE between matrix and reinforcement, is usually denoted as type II stress (like the so called inter-granular stress in single phase alloys) and the second one as type III stress. A detailed summary of the different types of internal stresses that can be developed in these composite materials can be found elsewhere [20,28]. Since the manufacture routes of MMCs always involve high temperature stages, the type II stress fields are such that the metallic matrix is in tension, whereas it is compressive in the reinforcement to balance the matrix tensile stress once the material is cooled down to room temperature. As mentioned in the introduction, these will not be referred to here to as residual, but as internal stress fields since they will undergo important variations during the thermal cycles, as it will be proposed.

On this basis, the different phenomena observed during composite thermal cycling, summarized in Figs. 4–7, can be understood from the way the different microscopic stress fields evolve and interact with the dislocations generated at the SiC-Al interface. We propose that the evolution of microscopic stresses (type II and III) during a given cycle occurs as schematically described in Fig. 8. Here, a linear dependence of temperature with time, both in the cooling and heating stages, is assumed for simplicity.

During the first period of the cooling stage, period t_0-t_1 in Fig. 8 (where $t = t_1$ is, say, a given arbitrary time instant during cooling), type II stress in the Al alloy phase increases until yielding occurs at t_1. Similarly, the corresponding stress in the reinforcement becomes negative, faster (in absolute value) than in the alloy due to its lower CTE and higher elastic modulus. When time t_1 is reached, local alloy yielding, *i.e.* dislocation generation, occurs, mainly at the near ends of the SiC_w. As it is known, dislocations are massively generated at metal-ceramic interface, mainly at whisker ends, during the cooling stage involved in the fabrication process of these MMCs. Proof of this is given in several studies which report TEM observations of this interface during cooling and heating *in situ* experiments [38–40]. This effect is due to the large difference between the CTE of the metallic matrix and the ceramic reinforcement, which obliges the matrix to yield beyond its elastic limit. On this way, the metallic matrix not only accumulates a tensile internal stress (while the stress in the ceramic is compressive), but also a large amount of dislocations, mainly at whiskers ends in agreement with [39]. As mentioned, detailed TEM studies have been conducted to show, *in situ*, the generation of dislocations during cooling of MMC materials [37]. The amount of dislocations generated by this process has been also the subject of detailed studies in the past [39]. We propose that these are mainly moving dislocations, which inhibit dislocation pinning effect for microstructural stabilization. Dislocation generation involves the appearance of type III internal stresses, consistently with [28]. Further cooling after t_1, in period t_1-t_2, type II stress (in the metallic and ceramic phases) increases, but it must occur at a lower rate than in period t_0-t_1. This is because the matrix keeps yielding, but it must occur now under local strain hardening, *i.e.* an associated increase of the dislocation density. Dislocation generation progresses as temperature continuous to decrease in this period, leading to an accompanying increase of the type III stress field. At the lowest temperature of the cycle, T_m at t_2 in Fig. 8, the maximum level (in absolute value) of the microscopic internal stresses, type II and III, must be attained.

During the subsequent heating period, the opposite phenomena must occur: The Al alloy phase expands faster than the ceramic one and the

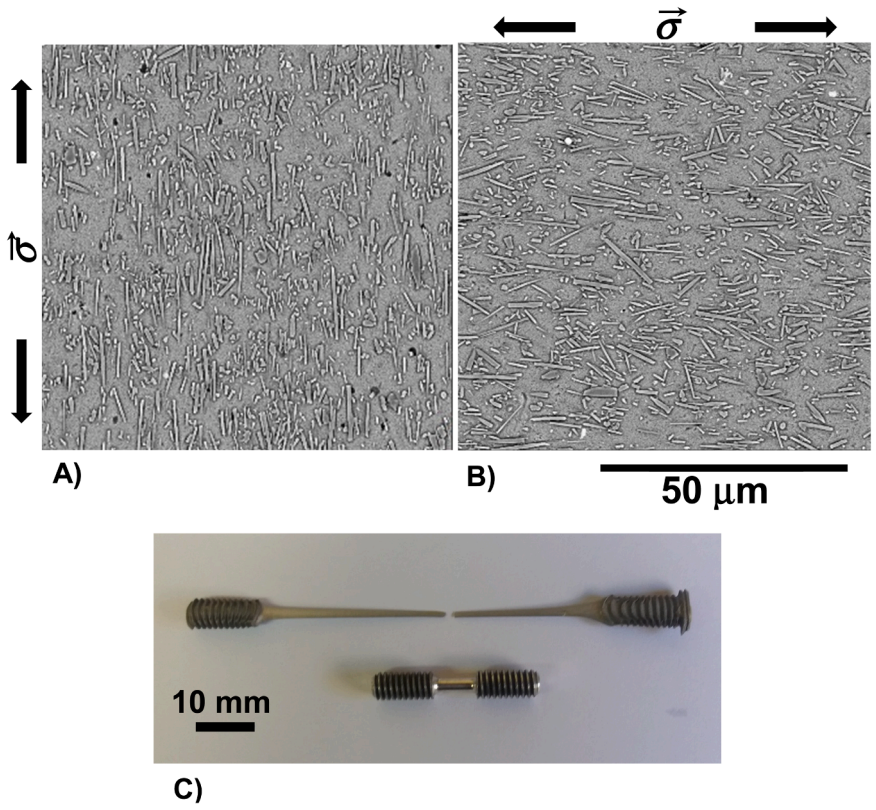

Fig. 6. Microstructure of the 6061Al-20vol%SiC_w composite material (section E-T) showing homogenization of the reinforcement due to thermal cycling and alignment with the external stress direction (indicated by arrows). A) Applied stress along E direction. B) Applied stress along T direction. C) Example of super-plasticity achieved, exceeding 1000% elongation, after thermal cycling under an external applied load.

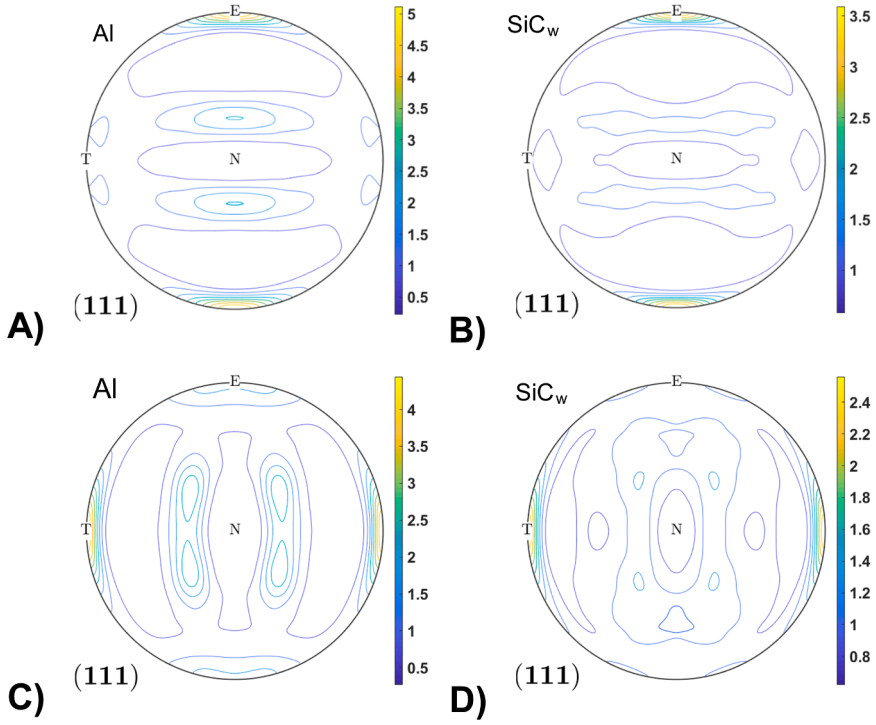

Fig. 7. Pole figures, (111), of thermally cycled samples under a uniaxial external applied stress along direction E for: A) the matrix phase and B) the SiC_w one, and direction T for: C) the matrix phase and D) the SiC_w one.

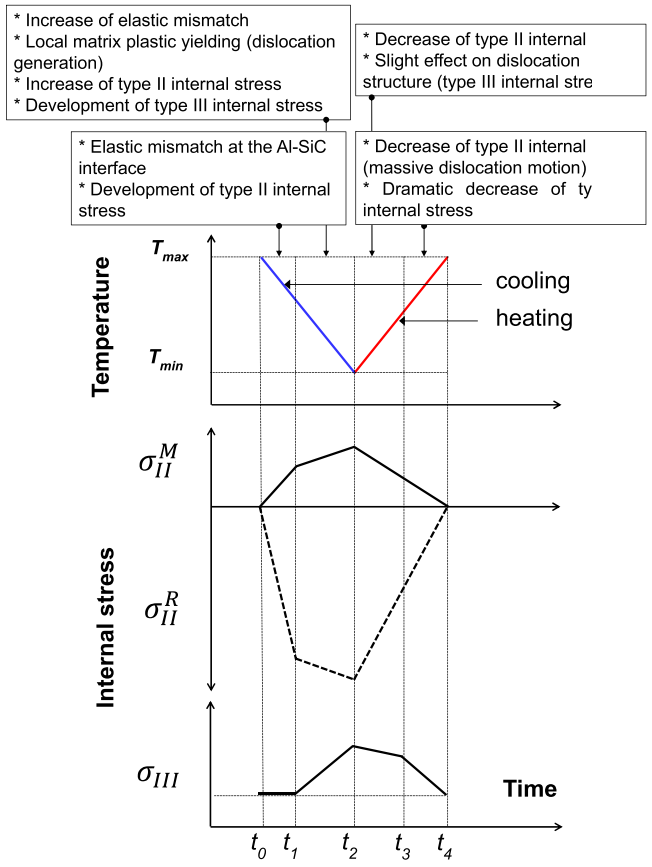

Fig. 8. Scheme indicating the way in which the microscopic internal stresses (type II and type III; σ_{II} and σ_{III} respectively) evolve during a given temperature cycle. For simplicity, a linear dependence of temperature on time, $T(t)$, during the cooling and heating periods of the cycle is assumed. Super-indexes M and R of the internal stresses denote matrix and reinforcement, respectively.

accumulated type II stress generated in both phases in period t_0-t_2 relieves progressively (in absolute value). In agreement with [38], the generation of dislocations of opposite sign to that of the dislocations generated during cooling should not occur. Instead, the dislocations must move, driven by the internal (an, if so, external) stresses until they disappear, with the consequence of a "net" plastic deformation of the sample. Assuming that in period t_2-t_3 the temperature is not high enough for local dislocation restoration/rearrangement phenomena and that type II stress does not affect the dislocation structure, type III stress must not be altered. Only a slight decrease associated with the decrease of elastic constants with temperature might occur. Once a high enough temperature is reached, say at $t = t_3$ in Fig. 8, local restoration phenomena, including dislocation motion, reorganization, and annihilation (towards possible sub-grain formation) should begin. This leads to a decrease in type III stress until the initial stress level is reached at $t = t_4$. This is, again, in agreement with the observed phenomenon of the disappearance of dislocations at high temperature in similar MMCs [39]. At this point, the microscopic stress field is the one associated with the remaining lattice defects, including the residual dislocation density. Here, at $t = t_4$, the maximum temperature of the cycle, T_M, is reached and type II internal stress may have vanished (the same stress level as in $t = t_0$ is attained). Assuming that the evolution of the dislocation density at SiC_w ends does not modify the contraction rate of the matrix/reinforcement phases, the rate at which type II stress decreases during period t_3-t_4 can be considered nearly constant, in agreement with the *in situ* TEM observations of Al-SiC MMC interface while heating [38,39]. The reversible character of the expansion/contraction processes of matrix and reinforcement which can be associated with the thermal cycles allows the evolution of these microscopic stress fields to be repeated during the successive cycles.

It is proposed that, in the absence of an external applied stress, the dislocation density (mainly formed by moving dislocations) generated in period t_1-t_2 is driven by type II stresses; dislocation motion during the period t_3-t_4 occurs in a way that their associated type III stress field gradients also decrease to minimize the local dislocation density. These gradients are initially established by the degree of inhomogeneity of the reinforcement distribution in the matrix, Fig. 2, and to the observation of dislocation generation mainly at SiC_w ends [40]. Therefore, dislocation motion in period t_3-t_4 should occurs in a way that the SiC_w reinforcing particles are "pushed" apart from each other to minimize the strain energy associated with the type III stress field; The closer the SiC_w are the higher the local dislocation density and the accompanying type III stress and internal strain energy. As it has been observed [40], the dislocations generated on cooling form tangles near the reinforcement and the distribution was seen not to be homogeneous; the dislocation density was higher in the vicinity of the SiC particles that at large distances from them. This explains the reinforcement homogenization and the increasing disorientation observed after thermal cycles, Figs. 4 and 5. Furthermore, dislocation motion in stage t_3-t_4 must occurs, to some extend, in a random manner. In this way the intensity of the initial β fiber type texture of the matrix must decrease with respect the initial one.

If an external tensile stress is also applied, the motion of the huge amount of moving dislocations in period t_3-t_4 is also affected by the external stress. Massive dislocation motion, driven mainly by this stress, occurs resulting in a macroscopic strain compatible with the tensile stress direction. Due to the extremely high elongation achieved in these conditions, matrix deformation obliges the un-deformable SiC_w to rotate towards the tensile axis direction, as also observed in [22]. Contrary to the case of only thermal cycles (no external stress) the strong fiber texture developed in the matrix phase is a consequence of a massive dislocation motion. As a result, the individual grains rotate the crystallographic ⟨111⟩ towards the tensile axes direction.

It is worth remarking on the very different deformation mechanism associated with the superplastic behavior observed here, Fig. 7, compared to the commonly accepted GBS mechanism in monolithic superplastic alloys [17–19]. Superplasticity in MMCs under thermal-cycling conditions occurs, as it has been demonstrated, as a result of the motion of a huge amount of dislocations. The dislocations are generated during the cooling period of the cycles at the metal-ceramic interface and they move, driven principally by the externally applied stress, during the heating period.

5. Summary

The texture and microstructural changes observed in 6061Al-20vol% SiC_w MMC during repeated thermal cycles, under the absence and the simultaneous action of an external tensile stress, are explained on the basis of the microscopic internal stress variations and the interaction of these stress fields with the dislocations generated during the cooling period of the thermal cycles. Temperature changes modify microscopic internal stress fields (type II and III). In the cooling period a large amount of moving dislocations is generated at the matrix-reinforcement interface, mainly at the near ends of the SiC_w (the interface "pumps" moving dislocations to the metallic matrix, inhibiting dislocation pinning phenomenon). During the heating period the dislocations move driven by the action of the type II stress fields, an interaction which must result in a non-directional collective dislocation motion. Reinforcement homogenization is observed and associated with a reduction of type III microscopic stress field gradients. The near random dislocation motion occurring during heating also reduces the texture intensity and type II stress becomes insignificant.

If a uniaxial external stress is also applied, the texture is accentuated, revealing that the motion of the large amount of dislocations is mainly

driven by the external stress, with little effect of the internal ones. Here, extremely large elongations can be achieved by a simple massive dislocation motion process. The motion of dislocations on their crystallographic systems obliges matrix grains to rotate the crystallographic ⟨111⟩ with the tensile axis direction.

Finally, the most significant finding that can be drawn from this research resides in the dramatic change of role that the SiC-Al interface must play during service at high temperature of these MMCs depending on the external conditions; When isothermal conditions prevail during component service, load transfer at the interface is the dominant underlying mechanism if the composite undergoes external stresses. This gives the material the superior mechanical properties, in comparison to the corresponding unreinforced alloy. However, when the external conditions involve severe and repeated temperature changes, the load transfer mechanism vanishes and, instead, a mobile dislocation pumping phenomenon operates at the interface. This confers the material a very high ductility (superplasticity), in particular when the external loads are very low. Therefore, it must be emphasized that for the design of structural components manufactured from MMCs, it is crucial to know the specific external stresses and temperature variation ranges under which they will operate. A dramatic change in the mechanical response must be expected if the temperature variations are excessive.

CRediT authorship contribution statement

ME, Microstructure and formal analysis. ILl, Texture experiments. RF and GGD model development. All, Discussions and draft preparation.

Declaration of Competing Interest

The authors declare that they have no known competing financial interests or personal relationships that could have appeared to influence the work reported in this paper.

Data Availability

The raw data required to reproduce these findings cannot be shared at this time due to technical limitations.

Acknowledgements

Projects Micro-Stress-MAP Y2018/NMT-4668 from Comunidad Autónoma de Madrid, and MAT2017-83825-C4-1-R and TECNOFUSIÓN (III)-CM S2018/EMT-4437, from MINECO, Spain.

References

[1 W.S. Miller, F.J. Humphreys, Strengthening mechanisms in particulate metal matrix composites, Scr. Met. 25 (1991) 33–38.
[2 R. Fernández, G. González-Doncel, Threshold stress and load partitioning during creep of metal matrix composites, Acta Mater. 56 (2008) 2549–2562.
[3] S. Spigarelli, C. Paoletti, A new model for the description of creep behaviour of aluminium-based composites reinforced with nanosized particles, Compos. Part A Appl. Sci. Manuf. 112 (2018) 346–355.
[4 J.K. Kim, P.K. Rohatgi, J.O. Choi, C.O. Choi, Wear properties and effect of molds on microstructure of graphite reinforced copper alloy composites made by centrifugal casting, Met. Mater. Inter. 11 (2005) 333–340.
[5 J. Corrochano, J.C. Walker, M. Lieblich, J. Ibáñez, W.M. Rainforth, Dry sliding wear behaviour of powder metallurgy Al-Mg-Si Alloy-MoSi2 composites and the relationship with the microstructure, Wear 270 (2011) 658–665.
[6 S. Rawal, Metal-matrix composites for space applications, JOM 53 (2001) 14–17.
[7 P.K. Rohatgi, D. Weiss, N. Gupta, Applications of fly ash in synthesizing low-cost MMCs for automotive and other applications, JOM 58 (2006) 71–77.
[8 S. Kumar, S. Ingole, H. Dieringa, K.-U. Kainer, Analysis of thermal cycling curves of short fibre reinforced Mg-MMCs, Comp. Sci. Technol. 63 (2003) 1805–1814.
[9 G. Daehn, G. González-Doncel, Deformation of whisker-reinforced metal matrix composite under changing temperature condition, Metall. Trans. 20A (1989) 2355–2368.
[10 H.D. Chandler, A composite model description of internal stress superplasticity, Mater. Sci. Eng. A 527 (2010) 2451–2454.
[11 S. Li, X. Ren, H. Hou, The effect of thermal cycling in superplastic diffusion bonding of 2205 duplex stainless steel, Mater. Des. 86 (2015) 582–586.
[12 S.M. Pickard, B. Derby, The deformation of particle reinforced metal matrix composites during temperature cycling, Acta Metall. Mater. 38 (1990) 2537–2552.
[13 S. Durieux, J.Y. Buffiere, G. Lormand, A. Rapoport, A. Vincent, Enhanced plasticity in metal matrix composites during thermal cycling under load, Mater. Sci. Eng. 234A (1997) 953–957.
[14 M. Kawasaki, T.G. Langdon, Review: Achieving superplastic properties in ultrafine-grained materials at high temperatures, J. Mater. Sci. 51 (2016) 19–32.
[15 G. González-Doncel, S.D. Karmarkar, A.P. Divecha, O.D. Sherby, Influence of anisotropic distribution of whiskers on the superplastic behavior of aluminium in a back-extruded 6061Al-20%SiCw composite, Comp. Sci. Technol. 35 (1989) 105–120.
[16 M.Y. Wu, O.D. Sherby, Superplasticity in a silicon carbide whisker reinforced aluminum alloy, Scr. Met. 18 (1984) 773–776.
[17 O.D. Sherby, J. Wadsworth, Superplasticity - Recent advances and future directions, Prog. Mater. Sci. 33 (1989) 169–221.
[18 M.T. Pérez Prado, M.C. Cristina, O.A. Ruano, G. González-Doncel, Grain boundary sliding and crystallographic slip during superplasticity of Al–5%Ca–5%Zn as studied by texture analysis, Mater. Sci. Eng. 244A (1998) 216–223.
[19 R. Fernández, M. Mabuchi, K. Higashi, G. González-Doncel, Texture evolution with superplastic deformation of a AlCu4Mg/Si3N4/20p composite, Comp. Sci. Technol. 69 (2009) 373–377.
[20 P.J. Withers, H.K.D.H. Bhadeshia, Residual stress, Part 1 – Measurement techniques, Mater. Sci. Technol. 17 (2001) 355–365.
[21 K. Kitazono, R. Hirasaka, E. Sato, K. Kuribayashi, T. Motegi, Internal stress superplasticity in anisotropic polycrystalline materials, Acta Mater. 49 (2001) 473–486.
[22 C. Schuh, D.C. Dunand, Whisker alignment of Ti-6Al-4V/TiB composites during deformation by transformation superplasticity, Int. J. Plast. 17 (2001) 317–340.
[23 M.T. Perez-Prado, G. González-Doncel, O.A. Ruano, T.R. Mcnelley, Texture analysis of the transition from slip to grain boundary sliding in a discontinuously recrystallized superplastic aluminum alloy, Acta Mater. 49 (2001) 2259–2268.
[24 M. Eddahbi, A. Borrego, M.A. Monge, G. González-Doncel, Microstructure after severe plastic deformation by torsion of powder metallurgy 6061 aluminum alloy, Mater. Sci. Eng. A555 (2012) 154–164.
[25 M. Eddahbi, T. McNelley, O.A. Ruano, Evolution of grain boundary character during superplastic deformation of an Al-6%Cu-0.4%Zr alloy, Metall. Trans. 32A (2001) 1093–1102.
[26 R. Hielscher, H. Schaeben, A novel pole figure inversion method: specification of The MTEX Algorithm, J. Appl. Crys. 41 (2008) 1024–1037.
[27 A. Borrego, R. Fernández, M.C. Cristina, J. Ibáñez, G. González-Doncel, Influence of extrusion temperature on the texture and the microstructure of 6061Al-15vol%SiCw PM composites, Comp. Sci. Technol. 62 (2002) 731–742.
[28 M.E. Fitzpatrick, P.J. Withers, A. Baczmanski, M.T. Hutchings, R. Levy, M. Ceretti, A. Lodini, Changes in the misfit stresses in an Al/SiCp metal matrix composite under plastic strain, Acta Mater. 50 (2002) 1031–1040.
[29 B.C. Kandpal, J. Kumar, H. Singh, Fabrication and characterization of Al2O3/aluminum alloy 6061 composites fabricated by stir casting, Mater. Today.: Proc. 4 (2017) 2783–2792.
[30 S. Li, Q. Zhao, Z. Liu, F. Li, A Review of Texture evolution mechanisms during deformation by rolling in aluminum alloys, J. Mater. Eng. Perform. 27 (2018) 3350–3373.
[31 M. Eddahbi, M. Carsí, O.A. Ruano, Characterization of a thermomechanically processed powder metallurgy Al-5%Mg-1.2%Cr alloy, Mater. Sci. Eng. A361 (2003) 36–44.
[32 J. Hirsch, K. Lücke, Mechanism of deformation and development of rolling textures in polycrystalline f.c.c. metals- I. Description of rolling texture development in homogeneous CuZn alloys, Acta Met. 36 (1988) 2863–2882.
[33 J. Hirsch, K. Lücke, Mechanism of deformation and development of rolling textures in polycrystalline f.c.c. metals- II. Simulation and interpretation of experiments on the basis of Taylor-type theories, Acta Met. 36 (1988) 2883–2904.
[34 F.J. Humphreys, M. Haltherly, "Recrystallization and related annealing phenomena", Chapter 9: "Recrystallization of Two Phase Alloys", Elsevier, 1996, pp. 285–319.
[35 J.-c Li, K.-b Nie, K.-k Deng, S.-j Shang, S.-s Zhou, F.-j Xu, J.-f Fan, Microstructure stability of as-extruded bimodal size SiCp/AZ91 composite, Mater. Sci. Eng. A615 (2014) 489–496.
[36 J. Geng, T. Hong, Y. Shen, G. Liu, C. Xia, D. Chen, M. Wang, H. Wang, Microstructural stability of in-situ TiB2/Al composite during solution treatment, Mater. Charact. 124 (2017) 50–57.
37 D. Liu, P.E.J. Flewitt, Raman measurements of stress in films and coatings, Spectrosc. Prop. Inorg. Organomet. Compd. 45 (2014) 141–177.
[38 C.Y. Barlow, N. Hansen, Dislocation configurations in metal-matrix composites correlated with numerical predictions, Acta Metall. Mater. 43 (1995) 3633–3648.
[39 M. Vogelsang, R.J. Arsenault, R.M. Fisher, An in situ HVEM study of dislocation generation at Al/SiC interfaces in metal matrix composites, Metall. Trans. 17A (1986) 379–389.
[40] R.J. Arsenault, N. Shi, Dislocation generation due to differences between the coefficients of thermal expansion, Mater. Sci. Eng. 81 (1986) 175–187.